Abbas, A, Carnacina, I, Ruddock, F, Alkhaddar, R, Rothwell, G and Andoh, R

The hydraulic performance of the storm chamber in a new manhole designed for separate sewer systems

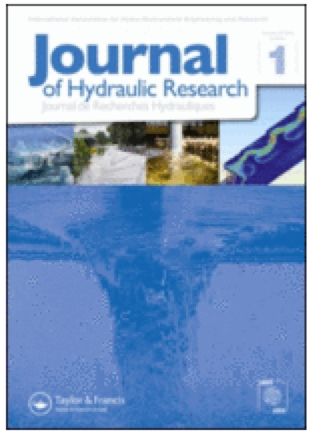

The hydraulic performance of the storm chamber in a new manhole designed for separate sewer systems

Journal:	*Journal of Hydraulic Research*
Manuscript ID	TJHR-2018-0210.R3
Manuscript Type:	Research paper
Date Submitted by the Author:	15-Oct-2019

Complete List of Authors:	Abbas, Alaa; Liverpool John Moores University, Civil Enginneering Carnacina, Iacopo; Liverpool John Moores University, Civil Engineering Ruddock, Felicity; Liverpool John Moores University, Civil Engineering Alkhaddar, Rafid ; Liverpool John Moores University, Civil Engineering Rothwell, Glynn; Liverpool John Moores University, Maritime and Mechanical Engineering Andoh, Robert ; AWD Consult Inc.

Keywords:	Dispersion flow, hydraulic structure design, manhole, separated flows, sewer hydraulics
JHR Keywords:	Hydraulic models < Instrumentation, measurements and experimental methods, Flow visualization and imaging < Instrumentation, measurements and experimental methods, Flow-structure interactions < Applied fluid mechanics and hydraulic engineering, Sewer hydraulics < Applied fluid mechanics and hydraulic engineering, Dispersion processes and models < Environmental Fluid Mechanics

Note: The following files were submitted by the author for peer review, but cannot be converted to PDF. You must view these files (e.g. movies) online.

Full flow 4ls-1-Conventional amnhole.MOV
βip over 0.5 - Flow of New Manhole.MOV
βip over 0.85 - Flow of New Manhole.MOV
βip over 1 - Flow of New Manhole.MOV

The hydraulic performance of the storm chamber in a new manhole designed for separate sewer systems

ALAA ABBAS (IAHR Member), Assistant Professor , *Department of Civil Engineering, Liverpool John Moores University, Liverpool, United Kingdom*
Email: A.H.Abbas@ljmu.ac.uk (*author for correspondence*)

IACOPO CARNACINA (IAHR Member), Assistant Professor, *Department of Civil Engineering, Liverpool John Moores University, Liverpool, United Kingdom*
Email: I.Carnacina@ljmu.ac.uk (*author for correspondence*)

FELICITY RUDDOCK, Programme Leader, *Department of Civil Engineering, Liverpool John Moores University, Liverpool, United Kingdom*
Email: F.M.Ruddock@ljmu.ac.uk

RAFID ALKHADDAR, Professor of Water and Environmental Engineering, *Head of the Department of Civil Engineering, Liverpool John Moores University, Liverpool, United Kingdom*
Email: R.M.Alkhaddar@ljmu.ac.uk

GLYNN ROTHWELL, Assistant Professor, *Department of Maritime and Mechanical Engineering, Liverpool John Moores University, United Kingdom*
Email: G.Rothwell@ljmu.ac.uk

ROBERT ANDOH, Professor, *CEO and President of AWD Consult Inc. 100 Tasha Circle, Ellenwood, GA 30294, United State of America*
Email: bandoh@awdconsult.com

Running Head: Hydraulic performance of a new manhole

The hydraulic performance of the storm chamber in a new manhole designed for separate sewer systems

ABSTRACT

This paper presents the hydraulic study of a new manhole geometry, designed to allow the installation of separate sewer systems in narrow streets. The new manhole design comprises two chambers in one structure to manage separate flows. The new shape of the manhole generates a new flow pattern for stormwater. It is therefore important to understand the hydraulic properties of sewer systems using the newly designed stormwater manhole chamber. The present study focuses on exploring the hydraulic performance of the storm chamber, which is usually characterized by significant head losses and shockwaves, these related to different flow regimes. A physical model was used to carry out a systematic experiment to explore the flow characteristics of the manhole under both subcritical and transitional flow conditions. The results revealed an enhancement in head loss with higher amplitude waves generated at transition flow when compared with a conventional manhole.

Keywords: Dispersion flow; hydraulic structure design; manhole; separated flows; sewer hydraulics.

1 Introduction

A manhole is one of the main elements of the sewer system, making it an important hydraulic structure that influences the hydraulic performance of the entire sewer network. Manholes are used to gain access to the sewer system to carry out cleaning, maintenance and inspection procedures, in addition to aerating the sewer system. They are positioned anywhere between 50 m and 100 m in the system or at any change in inlet or outlet pipe diameter, direction or level (Hager, 2010). Typically, separate sewer systems have two separate manholes: one for storm water flow and one for sewage flow. The sewage flow is easy to predict in comparison to stormwater flow, meaning that more attention needs to be paid to the design of the storm network in order to avoid the risk of flooding. The traditional separate sewer system requires a considerable amount of installation space, this making it a challenge for water companies when dealing with installations in narrow streets, these more common in the UK and EU (Broere, 2016; Marvin & Slater, 1997). A new design for a manhole has been developed in this research to overcome this challenge. The novel manhole includes two chambers: one for sewage flow and one for stormwater flow. The hydraulic performance of the storm chamber in the new manhole design differs from that of the conventional storm manhole for the traditional sewer systems as it generates a new pattern of stormwater flow inside the storm manhole chamber.

Sewers are normally designed to maintain free surface flow conditions using a pipe fill ratio of 85% (Gargano and Hager (2002) recommending 75%), this offering the same discharge capacity of a circular pipe under gravity flow. The flow in a sewer/manhole system is typically subcritical for Froude number (F) < 0.7, transitional for 0.7 < F < 1.5 and supercritical for F > 1.5 (Hager & Gisonni, 2005), depending on the pipe gradient and flow rate. When the filling ratio of a pipe is $\beta i_p =$ level of water at the inlet of the manhole (h_o)/ inlet pipe diameter (D_p) < 0.5, there is no shockwave at the outlet of the manhole. The transition, changing $\beta i_p > 0.5$, is associated with an interrupted flow which impinges on the outlet manhole (also known as flow choking), and changes the flow from free surface to pressurized air–water flow (Gargano & Hager, 2002). However, designing a storm sewer system with a prescribed filling ratio can be problematic, as there may be difficulties in accurately predicting rainfall intensity and the subsequent average quantity of inlet stormwater to the sewer network. Next to inherent design uncertainties, climate change can further exacerbate the correct design of a stormwater sewer. Transitional and supercritical flows are more common during wet seasons in storm networks or in combined networks. There have been no significant works to develop existing manhole designs, however, there have been many attempts to improve the hydraulic properties of the conventional manhole through the installation of extra accessories to enhance energy dissipation inside the manhole. A non-dissipated, upstream flow energy leads to high downstream flow velocity, this increasing the risk of flooding and erosion while also creating poor operating conditions (Granata, 2016).

Granata et al. (2014) investigated the hydraulic performance of drop manholes under supercritical flow conditions. They attempted to improve the hydraulic performance of the conventional drop manhole by installing a dissipative component i.e., two different types of jet-breaker; a plane jet-breaker and a wedge jet-breaker. Other studies have suggested adding control equipment by installing inlet flow restrictors in catchment basins, such as a Vortex Valve, and using these to limit inflow to the hydraulic capacity of the existing combined sewer system (Andoh et al., 2005). Increasing the flow path of storm water, reduces the height of shockwaves in the junction manhole or bend manhole, this associated with an increase in manhole storage capacity. Both these characteristics were identified through experimental tests conducted by Pfister and Gisonni (2014) for the junction manhole, and by Hager and Gisonni (2005) for the bend manhole. Froude number of approach flow (F_o) and filling ratios (βi_p) were used as parameters to describe the shockwaves inside the manhole. Saldarriaga et al. (2017) analysed the flow patterns of the symmetric junction in a manhole under supercritical flow conditions, recommending that improving the geometry could subsequently improve the hydraulic performance at the conventional junction manhole.

The new, streamlined manhole design presented in this paper, can improve the performance of a sewer network when compared to previous studies. The design uses a new manhole shape to reduce the footprint of the separate sewer system and to allow the installation of a separate sewer system where space is at a premium. It also increases the storage capacity of the stormwater chamber, extends the path of flow inside the chamber and creates an obstacle to the flow path through the presence of an internal wall. All these features can change the flow pattern of stormwater and increase the dispersion flow energy inside the storm manhole chamber. The subsequent hydraulic performance of the storm chamber in the new manhole was explored and compared with the hydraulic performance of a conventional manhole.

1.1 The new manhole design

The new manhole is cylindrical and has two chambers: the inner chamber is used as the conventional sanitary manhole, the external only used for storm water flow (Abbas et al., 2018). The level of the storm chamber is shallower than the sanitary chamber, the range of depth for both chambers changing according to the level of the inlet/outlet sanitary pipe for the inner chamber and the storm pipe for the outer chamber. In general, it is laid between 1 and 6 m below the road surface. This system requires the storm pipe to be located over the sanitary pipe. The diameter of the sanitary chamber can range from 0.7 to 1 m and the external chamber from 2.1 to 2.5 m, depending on the depth of the manhole. Figure 1 shows the design of the manhole and the separation technique.

2 Physical model

A physical model, an accepted approach used to establish an empirical method for designs or to simulate the flow in the manhole (Crispino et al., 2018), was used to run the experiments. All experiments were carried out in the civil engineering laboratory at Liverpool John Moores University, the aims to: i) explore the energy dispersion of storm flow through the new manhole under different flow rates when compared with the energy dispersion of storm flow through a conventional manhole; ii) to identify the shockwaves produced as a reaction to any alteration of the flow inside the storm chamber and, iii) to determine the velocity distribution at selected points. The physical model to prototype was scaled to 1/5, simulating the new combined manhole shape (Arao et al., 2012). The inner chamber was simulated by a 20 cm diameter Plexiglas pipe, the outer chamber 50 cm in diameter. Both chambers were fixed on one plane base and were 80 cm in length. The inlet pump with a maximum capacity adjustment flow rate of 8.5 l s^{-1}, was set in a water storage tank used to cycle flow water through the system. A flow meter was fixed next to and after the pump to measure the flow rate at a precision of 0.1 l s^{-1}. Two Plexiglas pipes were connected to the manhole's outer chamber as inlet outlet pipes. Both were10 cm in diameter and 1.5 m in length and equipped with two valves to control the flow rates and depth of flow. Three piezometers were fixed in the system to monitor the decrease in pressure through the model and energy losses. One was at the inlet pipe by the manhole, the second at the outlet pipe, the third at the start point of flow in the pipe after the pump (Fig 2a). A gate valve was placed upstream next to and after the pump to control the water level at the outlet pipe. A second gate valve was placed downstream after the manhole to control the F_o and βi_p at the inlet pipe. A camera was used to record the flow pattern and shockwaves under different flow rates. Two rulers were fixed in the new manhole, one on the external wall, the second on the internal wall to measure the amplitudes of the shockwaves. An OTT Z400 portable instrument, with an accuracy of ± 0.01 m s^{-1}, was used to measure the velocity at the inlet and outlet pipes as well as selected points inside the manhole. Head losses were compared with a conventional manhole by removing the inner sanitary chamber and using the external chamber as the conventional storm manhole model at a scale of 1/3. All other tools used for the new manhole are the same as those used to monitor the flow and head losses through the conventional manhole. Figures 2a and 2b show the setup of the physical model for the new manhole design.

2.1 Scale effects

A physical hydraulic model, which is either a smaller or larger scale, simulates the full-scale prototype. This is usually used to test any new design for optimization and investigate the operation under control conditions in a laboratory (Chanson, 2004). The physical hydraulic model can have scale effects if the scale ratio ≠ 1. In order to avoid scale effects between a physical scale model and a full-scale prototype, geometric similarity, kinematic similarity and dynamic similarity are required (Heller 2011).

In this study, an undistorted model has been used for the new manhole design. It has geometric similarity in that the same dimensions to scale were used for all components of the model. It also has kinematic similarity as the same direction of flow was used in addition to scale velocity between the physical model and prototype, at each corresponding point. Dynamic similarity requires the same ratios of inertial force to individual force components i.e. the Reynolds number (R_e), F and Weber number (W_e), at corresponding points between the physical model and prototype. This is can only be achieved by using the same scale for both the physical model and prototype or by using different types of fluid in both, neither of which are an economical nor practical solution (Chanson, 2004).

As such, Froude similitude, which is more appropriate for modelling a free-surface when the gravity effect is predominant and the flow is highly turbulent, is used in this study. The variation between Re, which is the inertial force to viscous force, and We which is the ratio of inertial force to surface tension between the physical model and the prototype, is associated with scale effects. The scale effects due to surface tension and viscosity can be negligible for the manhole when the $h_o \geq 0.04$ m (Crispino et al., 2018; Pfister and Gisonni, 2014) or when $R_e > 4000$ and W_e is small (Hamill, 2011).

Table 1 presents the ranges of dimensionless parameters used to characterize the flow for the physical model of the both manholes. The large-scale ratio (1/5) and turbulent flow in the model reduced these scale effects, this ratio of scale used by many researchers (Arao et al., 2012; Gargano & Hager, 2002; Granata et al., 2011; Stovin et al., 2008; Zhao et al., 2006).

2.2 The test program

Tests were programmed to use a variety of filling ratios (βi_p), starting from 0.25 up to 0.85 for a free-surface, the second set from free surface flow to full flow ($\beta i_p > 1$). Full flow is more common in a combined, or storm, network during heavy rain. The head loss (ΔH), under free-surface conditions and surcharge flow for both manholes, was monitored using dimensional variables such as inlet flow velocity (v), the diameters of both manhole and pipe (D_m and D_p), acceleration due to gravity (g) and the hydraulic gradient along the system (h_f, h_o, h_l and hg).

The head loss (ΔH) under free-surface conditions and surcharge flow for both manholes is mainly dependent on the following dimensional variable when discounting viscosity effects (R_e):

$$\Delta H = f\,(v, D_m, D_p, h_o, g) \tag{1}$$

The energy loss coefficient (K) is then expressed as a function of non-dimensional, independent variables which represent geometrical ratios as well as force ratios (Arao et al., 2012; Christodoulou, 1991), as shown in the equation below:

$$\frac{\Delta H}{\frac{v^2}{2g}} = f\left(\frac{h_o}{D_m}, \frac{h_o}{D_p} \frac{v^2}{gh_o}\right) \text{ meaning that } K = f(\beta i_m, \beta i_p, \mathsf{F}) \quad (2)$$

where v = mean pipe velocity; g = acceleration due to gravity, D_m = the manhole diameter, D_p = the inlet pipe diameter, h_o = the level of water at the inlet of the manhole, βi_p = the filling ratios of the inlet pipe, βi_m = the surcharge ratio of the manhole and K = the head loss coefficient.

It is assumed that the pipe slope is slight and that the pipe and manhole are circular. The same range of flow rates have been used for both manholes varying between 0.3 and 8.5 l s^{-1}, with an F_o between 0.2 and 0.9. The direct flow used for both manholes was without lateral connection and in total, 154 tests were conducted.

3 Results and discussion

The flow through conventional manholes was described by Hager and Gisonni (2005) who found that shockwaves were generated when the flow was over half the depth of the inlet pipe ($\beta i_p > 0.5$), this further reducing flow energy due to the friction of the flow created by the side walls. Choking occurs at the outlet manhole due to interrupted air-water flow, this resulting in more energy dissipation. Three shockwaves were determined in terms of basic hydraulic quantities for the conventional manhole: two inside the manhole and one at the outlet pipe. A revision of the filling ratio currently used in sewer designs has been recommended by Gargano and Hager (2002) in order for free-surface flow to be maintained at transitional and supercritical flow through the manhole and thus avoid flow choking. Energy flow dissipation inside the sewer manhole is required in many cases, specifically for combined systems or storm networks in a traditional separate sewer system. For example, the drop manhole is used to increase energy dissipation through sewer systems in hilly and mountainous regions for which the F is larger than 1.5 (velocity > 3 m s^{-1}) (Adriana Camino et al., 2014; Granata, 2016; Granata et al., 2011).

The new design of manhole here was designed to increase the head loss of stormwater flow through the storm chamber, in comparison to a conventional storm manhole, and to increase both the storage capacity and retention time of the flow inside the storm chamber. When proposing a new shape of manhole, the need emerges to explore the hydraulic features of the flow inside the new storm chamber and test its hydraulic integrity. Because the sewage water chamber has the same shape as the conventional manhole in the traditional system, the entire analysis focuses exclusively on the stormwater chamber. This section will first report on the analysis of the head loss coefficient for a different F_o and downstream boundary conditions, then attempt to quantify and study the shockwave amplitude, these results compared with the hydraulic performance of a conventional manhole.

3.1 Head losses through the new manhole

An analytical method was used to determine the head loss (*ΔH*) of flow inside the manhole from the difference of head pressure between the inlet and outlet of the manhole giving the coefficient of energy loss (Sangster et al., 1958).

$$\Delta H = K\frac{v^2}{2g} \quad (3)$$

The impact of the manhole geometry on the head loss coefficient has been simulated through a number of studies for specific shapes of manhole (Arao et al., 1999). The new manhole design generated a new path for the stormwater flow, as shown in Fig. 2b, where three points were found to disturb the flow and cause head losses in the storm chamber. The first point is the inner chamber wall, which blocks the storm flow path and splits it into two paths (ΔH_w); the second is at the two conduit bends inside the manhole (ΔH_b), the third the expansion and contraction at the entrance and outlet pipes, consequently (ΔH_e) and (ΔH_o).

ΔH_e and ΔH_o are at first approximation, similar to the head losses that occur in the entrance and outlet of the conventional storm manhole; the impact head loss at the entrance was limited by the distance equal to the diameter of the inlet pipe inside the manhole. This study is focused on the other two new head losses, ΔH_w and ΔH_b, generated from the new design of the manhole storm chamber. To simplify the calculation, it is assumed that the entrance and outlet head losses (ΔH_e and ΔH_o) are equal in both manholes, therefore calculated from the measurement of the head loss in a conventional manhole.

The head loss of flow through a conduit bend was investigated by Ito (1960). The head loss coefficient was derived using the ratio of the bend mid-radius, *R*, and the channel diameter, *D*, from one side, and the angle of curvature of the bend and the R_e from the other side. Ito's study showed that the minimum head loss coefficient occurred at $R/D = 2$ (Fig. 3), where ξ_k is the head loss as calculated in Eq. (3). The method used by Ito and the curves extracted from experimental works were applied to the new manhole design to calculate the head loss coefficient of the conduit bend. The new manhole is designed to have relative fixed dimensions between the inner chamber (sewage) and the outer chamber (stormwater) where the R/D ratio is 1.167 and the angle of curvature 45^0. The head loss coefficient was found to be approximately 0.1 for the corresponding velocity, equal to 1 m s^{-1} using Ito's (1960) chart. This is expected to be approximately twice that of the head loss coefficient which occurs at the curvature wall of the conventional manhole, as the new manhole design has two bends.

Experimental tests were conducted on both the new and conventional manhole design under the same boundary conditions, to identify the head loss generated from the obstacle to the storm flow path offered by the inner chamber wall (ΔH_w) in the new manhole design. ΔH_e and ΔH_o are the same in both manholes and can be identified from the calculation of the head loss in the conventional manhole. The ΔH_b of the new manhole is approximately twice the ΔH_b at the bend of the conventional manhole. When considering the independent dimensionless parameters for each manhole, Christodoulou (1991) stated that the local head loss in the manhole is essentially dependent on a dynamic parameter in the form of a F expressed in terms of flow velocity, the depth of flow and the geometrical characteristics. The head loss of the manhole is a function of diameter ratio (manhole diameter and pipe diameter) and the shape of the manhole (Pedersen & Mark, 1990). These parameters were used to characterize the hydraulic properties: (1) ratio of surcharge ($\beta i_m = h_o / D_m$), (2) F_o which are simplified by Hager (2010) for a circular channel, see Eq. (4) below, and (3) $\beta i_p = h_0 / D_p$

$$\mathsf{F}_o = \frac{Q}{\sqrt{g D_p h_o{}^4}} = \frac{Q}{\sqrt{g D_p{}^5 \beta i_p^4}} \tag{4}$$

where Q is the water discharge.

The experimental results showed that the flow was subcritical when $\mathsf{F} < 0.7$. Free-surface conditions were maintained when the depth of flow was less than 0.5 in the inlet pipe ($\beta i_p = h_0 / D_p <$ 0.5), changing to flow choking associated with shockwaves, when the flow transitioned from a free-surface to pressurized flow ($\beta i_p > 0.5$).

Figure 4 shows the comparison between the head loss coefficient generated in the new manhole, with the head loss coefficient of the conventional manhole under the same boundary conditions and at a different range of surcharge ratios (βi_m). The data shows a significant increase of flow energy dissipation (increasing in head coefficient) at a low βi_m for the new manhole when compared with the conventional manhole. This difference gradually decreased with an increase in surcharge ratio βi_m in both manholes until the flow transitioned from free-surface flow to pressurized flow, at approximately $\beta i_m = 0.33$ for the new manhole design and $\beta i_m = 0.2$ for the conventional manhole. The head loss coefficient tended to be constant under pressurized flow (full flow). The head loss coefficient of the conventional manhole fluctuates when the flow transfers from free-surface flow to full flow, while the head loss coefficient showed some stability in the new manhole design.

The head loss coefficient increases with an increasing filling ratio in the inlet pipe, for both manholes, when the filling ratio was below half the pipe diameter ($\beta i_p < 0.5$), as shown in Fig. 5. The comparison of data head loss coefficients for both manholes at different βi_p, illustrates the tendency of the head loss coefficient to decrease when the filling ratio is $0.5 < \beta i_p < 0.85$, dropping sharply at the transition between free-surface flow and pressurized flow. This coefficient tends to be constant after transitioning from a free-surface to pressurized flow ($\beta i_p > 1$). These results show the same behaviour as the data presented by Arao and Kusuda (1999) for a straight, conventional manhole without drops or changes in direction.

The head loss coefficient can be correlated to the non-dimensional dynamic momentum component ($\mathsf{F_o}.\beta i_p$) to extract preliminary design equations for both manholes. The data presented in Fig. 6, used to simulate the head loss coefficient with a non-dimensional dynamic momentum component, were used to fit Eq. (5), for the new manhole design, and Eq. (6), for the conventional manhole. The application of these two equations is limited to the specific dimension ratio between the inner chamber and external chamber as used in this research.

$$K_{ND} = 0.96(\mathsf{F_o}.\beta i_p)^{-0.65} \qquad (5)$$

$$K_0 = 0.75(\mathsf{F_o}.\beta i_p)^{-0.4} \qquad (6)$$

3.2 Shockwaves and choking in the new manhole design

With reference to Hager and Gisonni (2005), shockwaves involve a medium increase of flow depth beyond the shock front, while a hydraulic jump results in the collapse of the supercritical flow regime and a backwater effect. The pattern of flow for conventional manholes was investigated by Gargano and Hager (2002). Different types of waves were identified inside the manhole: i) the small shockwave resulting from the expansion at the manhole entrance and ii) at the outer manhole the flow impinges on the arc-shaped sides and the top wall, this resulting in a so-called swell wave and choking. The extended experiment in the current research allowed exploration of the main hydraulic features of the new manhole design, including shockwave profiles and variation of velocity. Hereafter, the focus is on the pattern of shockwaves generated from the presence of the inner manhole and changes in the flow path in the stormwater chamber in the new manhole, compared with that in the conventional manhole, for both subcritical and transitional flow conditions.

In the case of depth ratio $\beta i_p > 0.5$, the impingement of the transitional flow on the manhole wall generates shockwaves associated with swell; the heights and locations of waves in the conventional manhole were determined by Gargano and Hager (2002). The new manhole design presents four shockwave patterns inside the storm chamber, the locations of these shockwaves being *A*, *B*, *b* and *C* (where C is equivalent to shockwave *S* in the conventional manhole), as shown in Fig. 2b.

There are no shockwaves for the subcritical flow (F < 0.7) when the filling ratio is below half the inlet pipe ($\beta i_p < 0.5$), as shown in Fig. 7a. The first shockwave (*A*) appeared when the filling ratio was over $\beta i_p > 0.5$, as shown in Fig. 7b, and continued to be the main shockwave of the flow for $0.5 < \beta i_p < 0.85$. This main wave, results from the impingement of the direct flow of the inlet pipe on the inner manhole wall; it is a continuous wave noticed in the new design and associated with transitional flow. The second two symmetrical shockwaves propagated in the storm chamber, *B* and *b*, were generated from the change in the flow direction caused by the two bends in the storm chamber. When $0.5 < \beta i_p > 0.85$, these shockwaves were associated with low amplitude. The amplitude of these two shockwaves increased with an increase in βi_p, however, were less than shockwave A when $\beta i_p < 0.85$, as demonstrated in Fig. 7c and Fig. 7d. The generation of these two shockwaves is associated with the swing, or slushing phenomena, for the flow inside the storm chamber. When $\beta i_p > 0.85$, the amplitude of these shockwaves (*B* and *b*) increased to be higher than shockwave A, as illustrated in Fig. 7e and 7f. The characteristics of such waves (*B* and *b*) have been described in detail by Hager (2010) with reference to the flow in one bending channel inside a conventional manhole. The last wave, *C*, was generated from flow choking at the outlet manhole at $\beta i_p > 0.85$, as shown in Fig. 7g. The domain of swirls results from when the choking wave was less than that observed in the conventional manhole, as the *B* and *b* shockwaves were predominated on the *C* wave. The three shockwaves and choking together generate a significant swing wave observed in the storm chamber at transitional flow. Figures 8a and 8b present the pattern of flow recorded for the conventional manhole where it can be observed that there is no significant shockwave when the filling ratio is less than 0.5 (Fig. 8a). The choking wave (S) occurs in the conventional manhole when $0.6 < \beta i_p < 0.75$ (Fig. 8b) as described by Gargano and Hager (2002).

The general swing wave generated from the four shockwaves, was used to estimate the characteristic of the average wave amplitude inside the storm chamber of the new manhole design. The relatively high amplitude shockwaves $Y_i = (h_i\text{-}h_1) / h_1$, which vary with the non-dimensional dynamic momentum $\mathsf{F}_o.\beta i_p$, are used to quantify the pattern of shockwaves, where h_i is the wave amplitude observed in the manhole (Gargano & Hager, 2002). Figure 9 illustrates the Y_i over ($\mathsf{F}_o.\beta i_p$) relationship for both the conventional and new manhole. The experimental results illustrate how high amplitude shockwaves increase rapidly when the flow changes from free-surface flow to pressurized flow; the conventional manhole has smaller amplitude shockwaves. The main shockwave (choking wave) normally occurs at the transitions between free-surface flow and pressurized flow for the conventional manhole and increases with increased dynamic momentum. The swing of the waves recorded in the conventional manhole was less than in the new manhole design and attained a maximum $\mathsf{F}_o.\beta i_p > 0.5$. This then became constant for larger values of $\mathsf{F}_o.\beta i_p$ as the wave transitioned from 0.1 to 0.05 (De Martino, 2002). The fluctuation range and the location of the choking wave recorded in these experiments for similar βi_p, was comparable to the shockwave S, identified by Gargano and Hager (2002), in the conventional manhole. These relationships were quantified for both manholes using Eq. (7) for the new manhole and Eq. (8) for the conventional manhole.

$$Y_{i\,(ND)} = 0.12\ln(\mathsf{F}_o.\beta i_p) + 0.32 \qquad (7)$$

$$Y_{i\,(o)} = 0.03\ln(\mathsf{F}_o.\beta i_p) + 0.09 \qquad (8)$$

The high swing amplitude associated with the transitional flow in the new manhole design can cause damage to the manhole structure and decrease the hydraulic capacity of the manhole. As such, it is an important design parameter to be considered. The shockwaves generated increase the flow depth beyond the shock front. This phenomenon causes a decrease in discharge capacity and may result in geysering of storm water out of the manhole onto the street (Hager & Gisonni, 2005). Therefore, the experimental work was extended using the physical model, to test the amplitude of shockwaves when a breakdown occurs in the flow downstream of the model. The gate valve located downstream of the physical model (the valve after the manhole), was used to disturb the flow and generate a backwater effect. This data provides a better understanding of manhole flow behaviour and tests the hydraulic integrity of the new manhole.

The surcharge ratio (βi_m) of the new manhole and the conventional manhole can also be related to the amplitude of the shockwaves at a fixed flow rate and for a variety of flow rates at transitional flow. Figure 10 illustrates the impact of the surcharge ratio (βi_m) on the amplitudes of the shockwaves (Y_i) for the new manhole design. Maximum Y_i were observed generally at a low surcharge ratio for the transitional flow. The wave amplitudes decreased until close to zero, when the surface water level in the manhole was stable, with an increase of surcharge ratio (βi_m). The amplitude and swing of shockwaves are around zero when the surcharge ratio is approximately equal to the diameter of manhole D_m (surcharge ratio $\beta i_m = 1$). A reduction in shockwaves provides an appropriate safety factor to avoid high hydrostatic pressure loads inside the manhole generated from the swing of the wave at a high surcharge ratio, although this may create pressure flow conditions within the network. The storm chamber in the new manhole has a higher storage capacity and longer path for stormwater flow compared with the conventional stormwater manhole. The retention time results from the extended path of stormwater flow and an increase in the storm system upstream, improving the hydraulic performance of the storm network and decreasing flooding risks downstream of the network.

4 Conclusion

This research explored the hydraulic performance of a novel manhole design, focusing exclusively on the storm chamber. The novel shape of the manhole was designed to facilitate the installation of separate sewer systems in narrow streets which are prevalent in UK and EU cities. Experimental works were conducted to explore and quantify the hydraulic properties of the flow through the new storm chamber, comparing this with that of a conventional manhole. The head loss coefficient and the pattern of shockwaves were investigated for both manholes under the same conditions using the independent dimensionless parameters for each manhole: ratio of surcharge (βi_m), approach flow Froude numbers (F_o), and filling ratios (βi_p). The new manhole design generates higher head losses, about twice the head loss generated in a conventional manhole, at a low βi_m. The head loss for both manholes tends to be stable and maintains a lower constant value when the flow transitions from free-surface flow to pressurized flow (at high βi_m). The domains of generating the head loss for the flow inside the storm chamber were determined; the inner chamber wall, the two conduit bends inside the manhole and the expansion and contraction at the entrance and outlet pipes. Four shockwaves were identified in the storm chamber of the new manhole design: (1) Shockwave *A* results from impingement of the direct flow of the inlet pipe on the inner manhole wall; (2 & 3) *B* and *b* were generated from the change in the flow direction caused by the two bends in the storm chamber and (4) shockwave *C* was generated from flow choking at the outlet manhole. The locations of these shockwaves were determined and the average amplitude of swing generated from the combined effects of these shockwaves quantified with non-dimensional dynamic momentum $F_o.\beta i_p$. The results showed a significant increase in shockwave amplitude in the new manhole design when the flow changed from free-surface to pressurise flow, this increasing the risk of failure in manhole performance. Therefore, the hydraulic integrity of the storm chamber in the new manhole was tested by breaking up the flow downstream of the model. The experimental results illustrated that the amplitude and swing of shockwaves decreases with an increase in the surcharge ratio (βi_m), this suggesting that the manhole design is safe in terms of structural damage and geysering phenomena associated risks. The study used a fixed dimensions ratio between the inner and outer chambers, and one coaxial configuration of the inner manhole located inside the outer chamber. The research can be developed to test a full-sale manhole insitu which allows to measure the scale effects on the flow properties and to develop a computational fluid dynamic model (CFD) to explore different configurations of the new manhole design.

Acknowledgements:

The authors would like to acknowledge the United Utilities Group PLC for providing technical support. The first author would like to acknowledge Al Ghalowa Co Ltd. for supporting this study. A special acknowledgement is for the technical staff of LJMU for their assistance with the experimental set-up.

Funding:

There has been no significant financial support for this work that could have influenced its outcome.

Supplemental data

This paper included supplemental material. Video clips show flow patterns and shockwaves generated at each corresponding flow rate for the new manhole design and for the conventional manhole.

Notation

A, B, b and C = shockwaves generated in the new manhole (-)

D_m = manhole diameter (m)

D_p = approach pipe diameter (m)

F = Froude number (-)

F_o = approach Froude number (-)

$\mathsf{F}_o.\beta i_p$ = non-dimensional dynamic momentum component

g = gravity acceleration (m s^{-2})

h_f = level of water at the beginning of inlet pipe (m)

h_g = level of water at the outlet of manhole (m)

h_i = level of amplitude of water in the manhole (m)

h_l = level of water in the manhole (m)

h_o = level of water at inlet of the manhole (m)

K_o = head loss coefficient (-), K_{ND} for the new manhole design and K_o for the conventional manhole

Q = discharge (m^3 s^{-1})

R = the bend mid-radius (m)

R_e = Reynolds number (-)

S and E = shockwaves generated in the conventional manhole (-)

Y_i = shockwaves amplitudes (-), $Y_{i\,(ND)}$ for the new manhole design and $Y_{i\,(o)}$ for the conventional manhole.

β_{im} = ratio of surcharge for the manhole (-)

β_{ip} = filling ratio in the approach pipe (-)

ΔH = head loss (m)

v = mean pipe velocity (m s^{-1})

W_e = Weber number (-)

References

Abbas, A., Ruddock, F., Al Khaddar, R., Rothwell, G., & Andoh, R. (2018). Improving the Geometry of Manholes Designed for Separate Sewer Systems. *Canadian Journal of Civil Engineering*, , *46*(1), 13-25.

Adriana Camino, G., Zhu, D. Z., & Rajaratnam, N. (2014). Flow observations in tall plunging flow dropshafts. *Journal of Hydraulic Engineering, 141*(1), 06014020.

Andoh, R. Y. G., Stephenson, A. J., & Collins, P. (2005). Approaches to Urban Drainage Systems Management for The 21 st Century. In *National Hydrology Seminar*.

Arao, S., Kusuda, T., Moriyama, K., Hiratsuka, S., Asada, J., & Hirose, N. (2012). Energy losses at three-way circular drop manholes under surcharged conditions. *Water Science and Technology, 66*(1), 45-52.

Arao, S., Mihara, T., & Kusuda, T. (1999). An optimal design method of storm sewer network considered with manhole energy loss. *Doboku Gakkai Ronbunshu, 1999*(614), 109-120.

Broere, W. (2016). Urban underground space: Solving the problems of today's cities. *Tunnelling and Underground Space Technology, 55*, 245-248. doi:https://doi.org/10.1016/j.tust.2015.11.012

Chanson, H. (2004). *Hydraulics of open channel flow*: Elsevier.

Christodoulou, G. C. (1991). Drop manholes in supercritical pipelines. *Journal of Irrigation and Drainage Engineering, 117*(1), 37-47.

Crispino, G., Pfister, M., & Gisonni, C. (2019). Supercritical flow in junction manholes under invert-and obvert-aligned set-ups. *Journal of Hydraulic Research*, , *57*(4), 534-546.

Gargano, R., & Hager, W. H. (2002). Supercritical Flow across Sewer Manholes. *Journal of Hydraulic Engineering, 128*(11), 1014-1017. doi:10.1061/(ASCE)0733-9429(2002)128:11(1014)

Granata, F. (2016). Dropshaft cascades in urban drainage systems. *Water Science and Technology*, *73*(9), 2052-2059.

Granata, F., De Marinis, G., & Gargano, R. (2014). Flow-improving elements in circular drop manholes. *Journal of Hydraulic Research, 52*(3), 347-355. doi:10.1080/00221686.2013.879745

Granata, F., de Marinis, G., Gargano, R., & Hager, W. H. (2011). Hydraulics of Circular Drop Manholes. *Journal of Irrigation & Drainage Engineering, 137*(2), 102-111. doi:10.1061/(ASCE)IR.1943-4774.0000279

Hager, W. H. (2010). *Wastewater Hydraulics Theory and Practice*. Springer Science & Business Media.

Hager, W. H., & Gisonni, C. (2005). Supercritical flow in sewer manholes. *Journal of Hydraulic Research, 43*(6), 660-667. doi:10.1080/00221680509500385

Hamill, L. (2011). *Understanding hydraulics*. Macmillan International Higher Education.

Ito, H. (1960). Pressure losses in smooth pipe bends. *Journal of Basic Engineering, 82*(1), 131-140.

Marvin, S., & Slater, S. (1997). Urban infrastructure: the contemporary conflict between roads and utilities. *Progress in Planning*, *4*(48), 247-318.

Pedersen, F. B., & Mark, O. (1990). Head losses in storm sewer manholes: submerged jet theory. *Journal of Hydraulic Engineering, 116*(11), 1317-1328.

Pfister, M., & Gisonni, C. (2014). Head losses in junction manholes for free surface flows in circular conduits. *Journal of Hydraulic Engineering, 140*(9), 06014015.

Saldarriaga, J., Rincon, G., Moscote, G., & Trujillo, M. (2017). Symmetric junction manholes under supercritical flow conditions. *Journal of Hydraulic Research, 55*(1), 135-142. doi:10.1080/00221686.2016.1212410

Sangster, W. M., Wood, H. W., Smerdon, E. T., & Bossy, H. G. (1958). Pressure changes at storm drain junctions.

Stovin, V. R., Guymer, I., & Lau, S. D. (2008, August). Approaches to validating a 3D CFD manhole model. In *11th international conference on urban drainage* (pp. 1-10).

Zhao, C.-H., Zhu, D. Z., & Rajaratnam, N. (2006). Experimental Study of Surcharged Flow at Combining Sewer Junctions. *Journal of Hydraulic Engineering, 132*(12), 1259-1271. doi:10.1061/(ASCE)0733-9429(2006)132:12(1259)

List of tables

List of figures

Acknowledgements: Reprinted by permission from [Springer Nature]: (Wastewater Hydraulic Book, Losses in Flow chapter, Willi H. Hager, 2010).

Figure 10 The wave amplitude (Y_i) at different surcharge ratios (βi_m) for the flow in the new manhole design at different flow rates.

Table 1. Experimental range of main dimensionless parameters

Manhole	βi_m	βi_p	F_o	R_e		W_e	
				model	prototype	model	prototype
New design	0.1 – 0.5	0.3 – 1.5	0.25 – 0.9	9500 - 71500	21500 -167000	0.1 - 0.9	0.4 - 5.0
Conventional	0.05 – 0.3	0.2 – 1.3	0.4 – 0.9	15000 - 72000	34000 - 180000	0.2 - 1.0	0.7-5.0

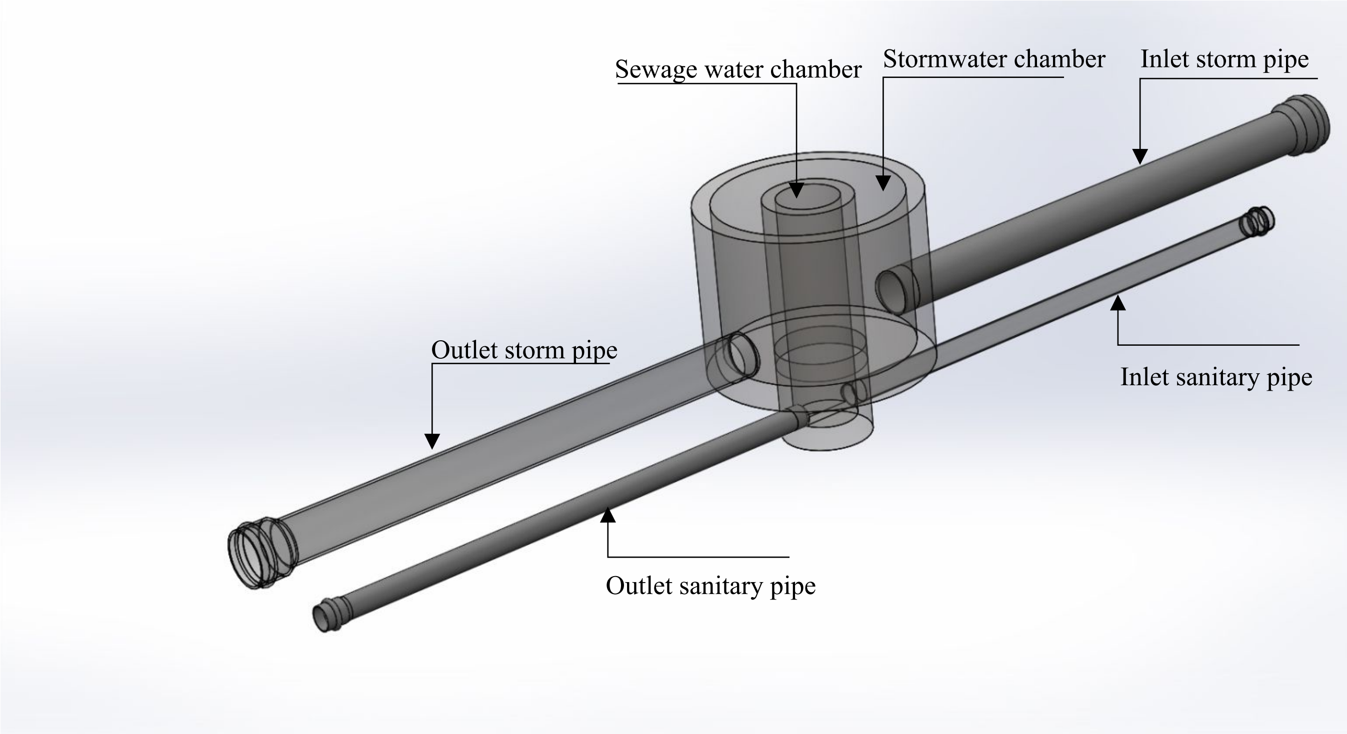

Figure 1 3D design of the innovative manhole.

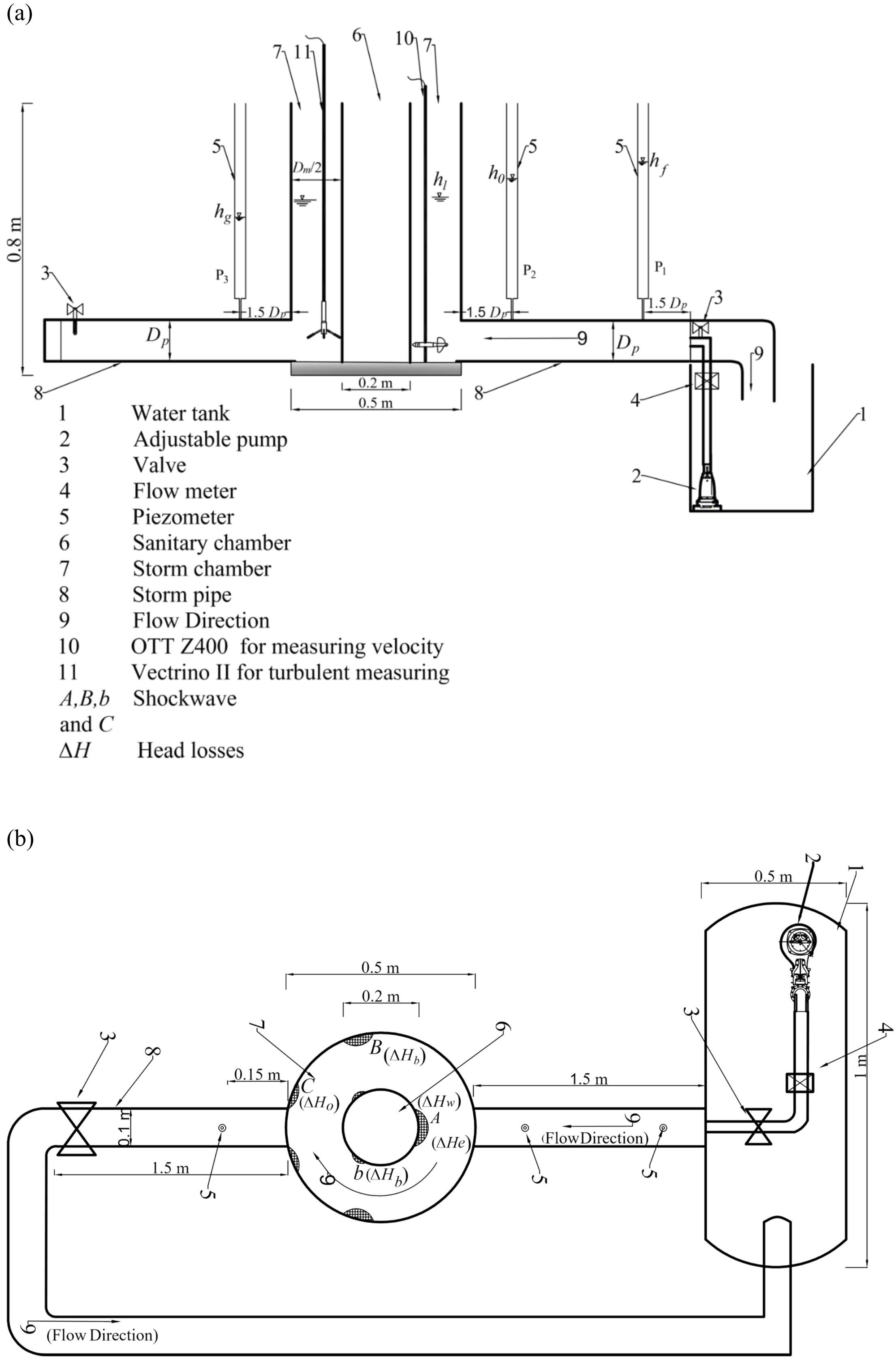

Figure 2 The physical model to test the hydraulic properties for the new manhole design (a) a cross section (b) a top view shows the location of shockwaves.

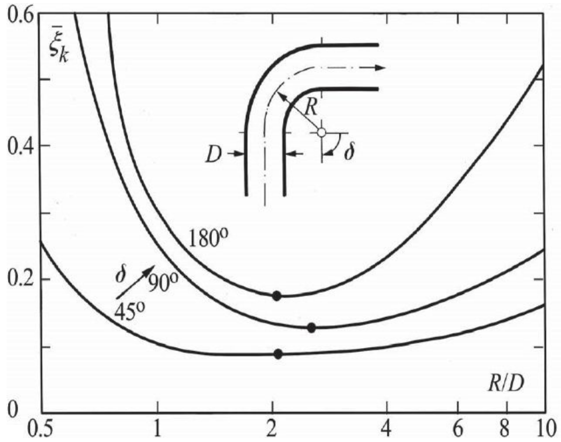

Figure 3 Total loss coefficient as a function of relative bend radius R/D and angles of curvature δ for $\mathsf{R_e} \geq 10^6$ (Hager, 2010).

Acknowledgements: Reprinted by permission from [Springer Nature]: (Wastewater Hydraulic Book, Losses in Flow chapter, Willi H. Hager, 2010).

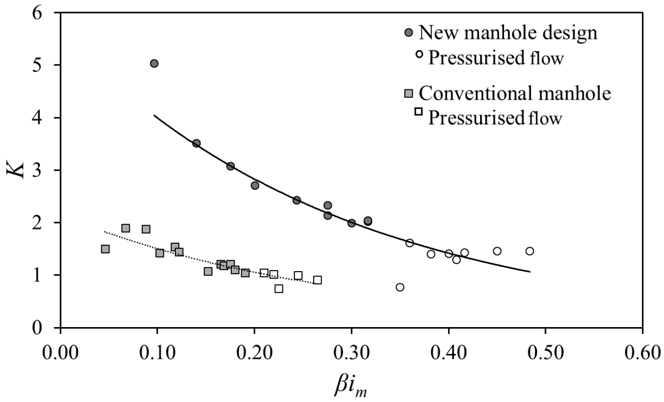

Figure 4 A comparison between the head loss of the new manhole design and conventional manhole at different surcharge ratio (βi_m).

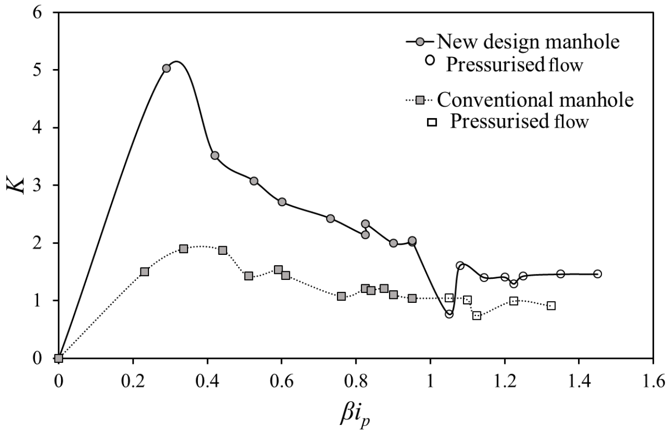

Figure 5 A comparison between the head loss of the new manhole design and the conventional manhole at different filling ratios (βi_p).

.

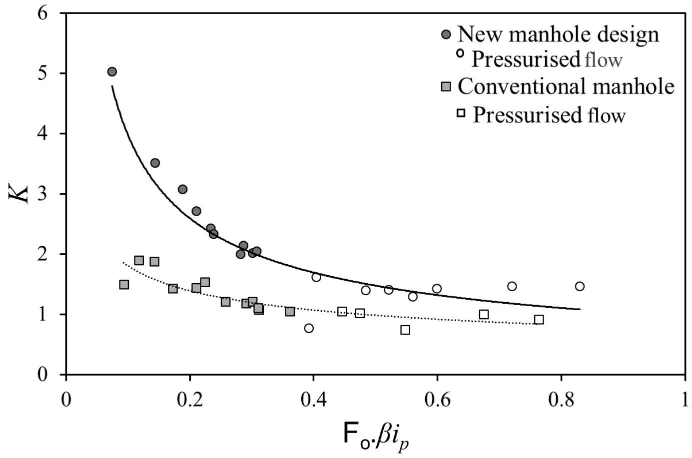

Figure 6 Relationship between the head loss coefficient and the non-dimensional dynamic momentum component ($\mathsf{F}_o.\beta i_p$) for the new manhole design and the conventional manhole.

(a)

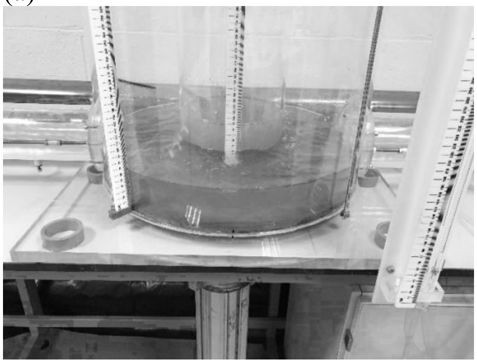

(b)

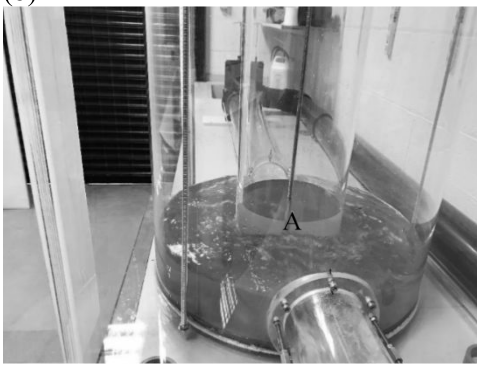

(c)

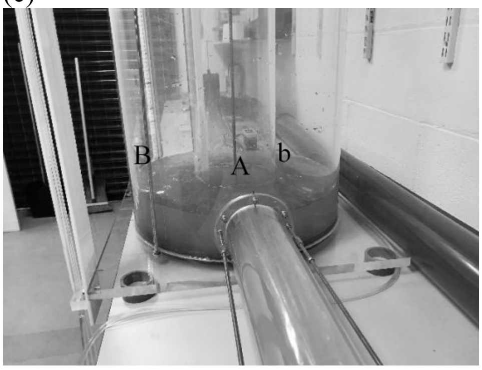

(d)

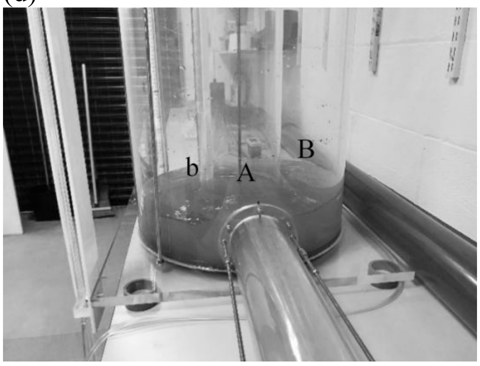

(e)

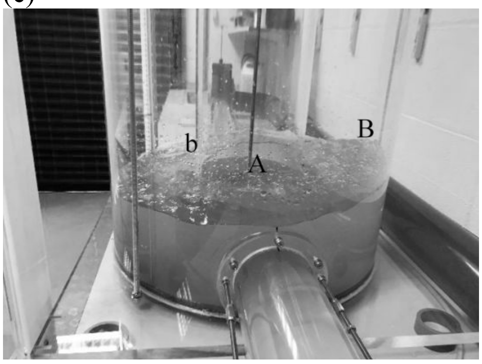

(f)

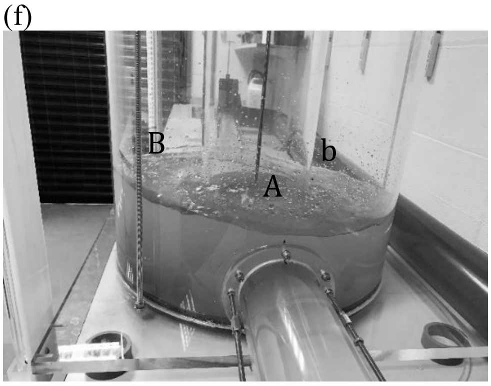

(g)

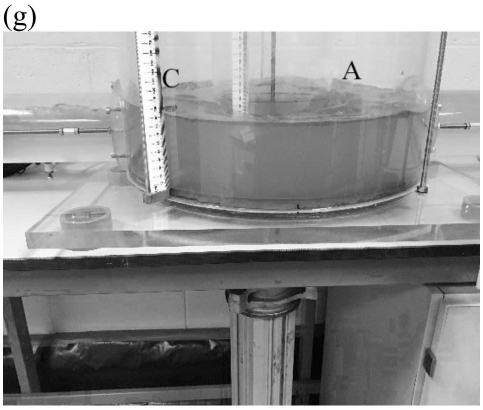

Figure 7 The pattern of shockwaves generated in the conventional manhole design at different filling ratios (βi_p) (a) No significant shockwave noticed when the filling ratio $\beta i_p < 0.5$ (b) The first and main shockwave (A) appeared when $\beta i_p > 0.5$ (c) The second shockwave B associated with (A) appeared when $0.5 < \beta i_p < 0.85$, but A is still the main shockwave (d) Swing phenomena appeared when $0.5 < \beta i_p < 0.85$ (e) Shockwave B and b are larger than shockwave A when $\beta i_p > 0.85$ (f) Shockwave B and b are larger than shockwave A when $\beta i_p > 0.85$ is associated with an increase in the swing phenomena (g) Shockwave B and b are larger than shockwave A when $\beta i_p > 0.85$.

(a)

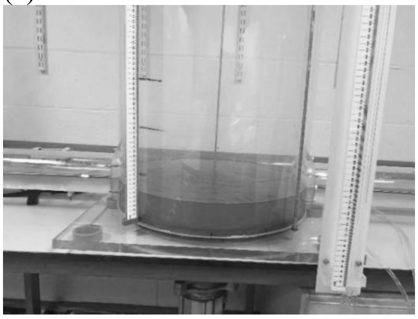

(b)

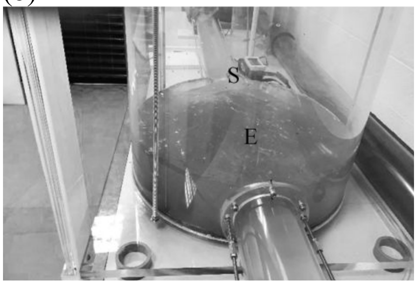

Figure 8 The pattern of shockwaves generated in the conventional manhole design at different filling ratios (βi_p) (a) The flow pattern for the conventional manhole under filling ratio $\beta i_p < 0.5$: there is no shockwave (b) The flow pattern for the conventional manhole under filling ratio $\beta i_p > 0.5$: shockwave S is generated.

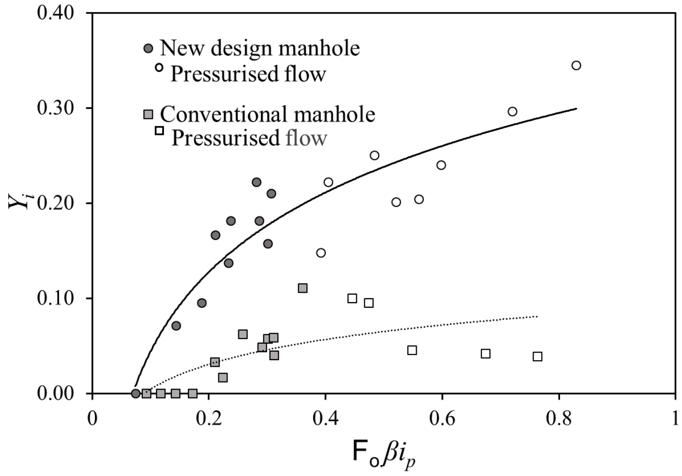

Figure 9 The amplitude of the average shockwaves (Y_i) against non-dimensional dynamic momentum ($F_o.\beta i_p$) for both the conventional and the new manhole design.

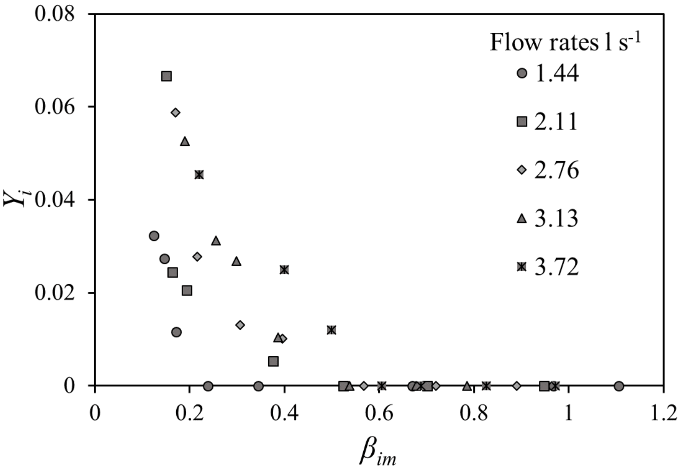

Figure 10 The wave amplitude (Y_i) at different surcharge ratios (βi_m) for the flow in the new manhole design at different flow rates.

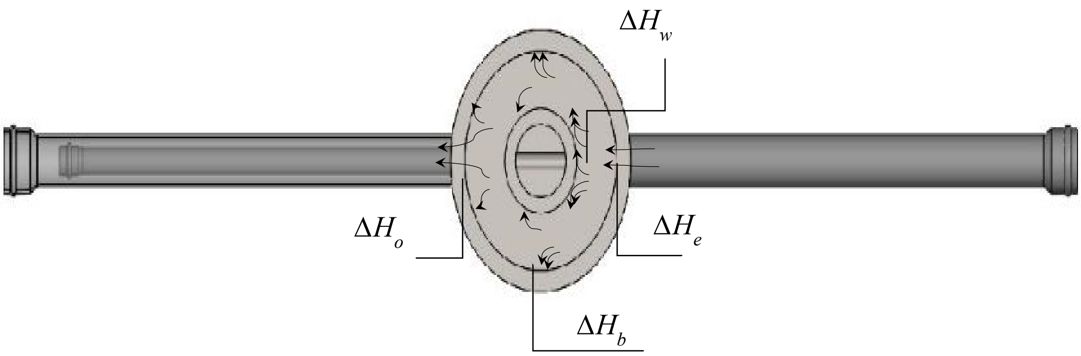

Figure 1 (supplementary) Top view of the new manhole design showing the storm flow path and three points of the head losses generated inside the storm chamber.